https://doi.org/10.5194/egusphere-2026-359
Preprint. Discussion started: 29 January 2026

Water mass modification of the warm Atlantic Inflow towards the Arctic across the Iceland-Faroe Ridge

Guðrið Eriksdóttir[1], Bogi Hansen[1], Karin Margretha H. Larsen[1], Steffen M. Olsen[2], Andrea M. U. Gierisch[2], Sólveig R. Ólafsdóttir[3]

[1]Faroe Marine Research Institute, Tórshavn, Faroe Islands
[2]Danish Meteorological Institute, Copenhagen, Denmark
[3]Marine and Freshwater Research Institute, Hafnarfjörður, Iceland

Correspondence to: Guðrið Eriksdóttir (gudridj@hav.fo)

https://doi.org/10.5194/egusphere-2026-359
Preprint. Discussion started: 29 January 2026

Abstract. The warm Atlantic inflow across the Iceland-Faroe Ridge (IFR) is the strongest of the three branches carrying warm water to the Nordic Seas and further into the Arctic. This branch (IF-inflow) carries almost 50 % of the total Atlantic water inflow. The Atlantic water crossing the IFR mainly flows through the Iceland Basin with no indication of a significant contribution from the Rockall Trough. The salinity variations of the Atlantic water approaching the IFR are well explained as a delayed response to the intrusion of the Subpolar Gyre into the Iceland Basin while the temperature variations may be seen as a combined response to the gyre and global warming. The flow corridor feeding the IFR with Atlantic Water gets narrower and migrates southeastward to the rim of the Iceland Basin when the Subpolar Gyre extends into the basin. As the Atlantic water crosses the IFR, it is cooled by at least 1 °C and freshened by at least 0.1 g kg^{-1}. Satellite-tracked drifters that crossed the IFR exhibited prolonged residence times on the western flank of the IFR together with a high level of eddy kinetic energy. This indicates that transformation occurs in this area. We show that transformation of the water mainly is caused by mixing with Arctic water masses, rather than by air-sea-interactions, and that most of the modification takes place upstream of the ridge crest. The Atlantic water changes character from an almost barotropic to a much more baroclinic flow over and northeast of the ridge enabling water masses, otherwise constrained to follow isobaths, to cross the ridge. We find that the cooling and freshening of the Atlantic water across the IFR are relatively constant throughout the whole period from 1993 to 2023, except for the last few years. The associated freshening implies that the salinity difference between IF-inflow water and the deep waters northeast of the ridge has been reduced by roughly 20–30 % after crossing the ridge, which weakens the potential for dense-water formation. Updated transport estimates show a slight strengthening for this AMOC branch. From 1993 to 2023, the volume transport of the IF-inflow increased by (12±7) %, while the heat transport relative to 0 °C increased by (16±8) %.

https://doi.org/10.5194/egusphere-2026-359
Preprint. Discussion started: 29 January 2026

1. Introduction

The exchange of water between the North Atlantic and the Arctic Mediterranean (Nordic Seas and Arctic Ocean with shelves) plays a central role in both the global and the regional climate. Through a complex system of currents, warm, saline water of Atlantic origin flows into the Nordic Seas from the North Atlantic. During its further journey through the Arctic Mediterranean, most of the Atlantic water is transformed into a denser water mass that can sink due to buoyancy loss (Østerhus et al., 2019). The subsurface Greenland-Scotland Ridge (GSR), extending from Greenland to Scotland via Iceland and the Faroe Islands (Faroes), acts as a barrier between the deep waters on either side. This cold, dense water fills up the basins north of the ridge and sets up pressure gradients across it. The deep water flows over the ridge at its deepest parts towards the Equator. This is the overflow. Conservation of mass dictates that water must then flow poleward in the upper layer. This is the Atlantic inflow. South of the GSR, the overflow water sinks to deeper levels as it entrains ambient waters.

This exchange of warm, saline water in the upper layer towards the Nordic Seas and cold, dense but less saline water at depth towards the Atlantic Ocean is the northernmost component of the Atlantic Meridional Overturning Circulation (AMOC), which transports heat poleward. Furthermore, the dense water that sinks transports excess heat and carbon from the surface to the deep ocean (Buckley and Marshall, 2016). According to the IPCC's 6th Assessment Report, the AMOC is very likely to decline over the 21st century (Arias et al., 2021), making it critical to understand the processes that regulate it.

Three main branches carry warm water to the Nordic Seas: the Denmark Strait inflow, the Faroe-Scotland inflow, and the inflow across the Iceland-Faroe Ridge (IFR). Østerhus et al. (2019) estimate the total Atlantic inflow across the GSR to be approximately 8 Sv. The strongest of these branches by volume, carrying 3.8 ± 0.5 Sv or 48 % of the total flow, is the branch across the IFR (Hansen et al., 2015, 2023), the IF-inflow, which is the focus of this study. Figure 1 shows the study region where the warm Atlantic water meets the cold Arctic water just north of the IFR in the Iceland-Faroe Front.

Hydrographic investigations of the waters at the IFR were initiated as early as in the 19th century (Knudsen, 1898) and have continued ever since, with much of the early studies reviewed by Hansen and Østerhus (2000). The main focus of almost all of these studies has, however, been on the formation of overflow water in the frontal zone and the overflow across the ridge. Despite this overflow-focus, considerable information has been gained on the temperature and salinity of the Atlantic water over and around the IFR.

In the mid-1990s, efforts were initiated to combine the hydrographic observations with velocity observations in order to generate time series of transport. The IFR is around 300 km wide and deeper than 300 m with a sill depth of around 480 m close to the Faroes. Furthermore, the IF-inflow occurs over most of the length of the ridge, but likely with large temporal and spatial variations (Childers et al., 2014; Hansen et al., 2023). A high fishing activity (trawling) endangers any moorings deployed on the ridge. Instead of monitoring the transport of IF-inflow over the ridge, it was therefore decided (Hansen et al., 2003) to monitor it at the N-section north of the Faroe Islands. This is possible due to the pathway of the IF-inflow. The Atlantic water that crosses the IFR meets fresher and colder water at the Iceland-Faroe Front, which is topographically locked

https://doi.org/10.5194/egusphere-2026-359
Preprint. Discussion started: 29 January 2026

to the ridge (Fig. 1). Here, the Atlantic water turns southeast and accelerates into a relatively narrow boundary current, the Faroe Current (Rossby et al., 2009; Hansen et al., 2010), which is easier to monitor.

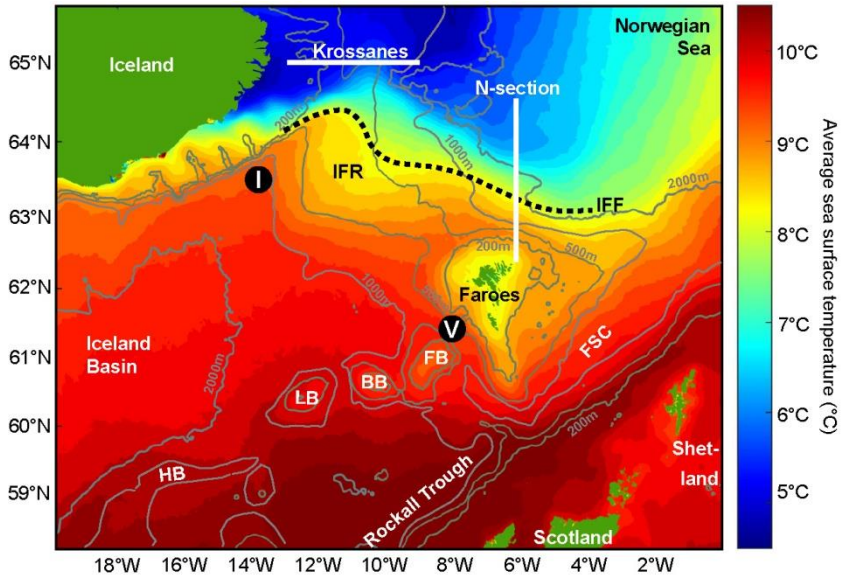

Figure 1. The colours indicate average sea surface temperature (SST) based on remotely sensed monthly SST maps in the period 2003–2020 (NASA Goddard Space Flight Center, Ocean Ecology Laboratory, Ocean Biology Processing Group). Two standard stations I and V (black circles) and two standard sections, the N-section and the Krossanes section (white lines) are shown. Isobaths are shown for 200 m, 500 m, 1000 m and 2000 m depth. IFR: Iceland-Faroe Ridge. FSC: Faroe-Shetland Channel. HB: Hatton Bank. LB: Lousy Bank. BB: Bill Baileys Bank. FB: Faroe Bank. IFF: Iceland-Faroe Front.

The N-section has been sampled two to six times annually by hydrographic cruises since the late 1980s. Since 1997, this has been complemented by an array of moored Acoustic Doppler Current Profilers (ADCPs), deployed below the extent of fishing gear or in trawl-protected frames on the bottom. By combining this information with data from satellite altimetry, a system has been established that allows monitoring of the volume transport of the Atlantic water flowing through the N-section as well as its heat transport relative to 0 °C (Hansen et al., 2023).

This monitoring has documented that this branch of the AMOC has not weakened since 1993 (Hansen et al., 2023) and we present updated transport values supporting earlier indications of strengthened flow. The focus of this manuscript is, however, not on the transport of the IF-inflow, but rather on its hydrographic properties. The monitoring system generates annual values for transport-weighted temperature and salinity for the Atlantic water passing through the N-section. These values represent the properties of the water continuing further into the Arctic Mediterranean.

The main aim of this manuscript is therefore to explain the temperature and salinity of the Atlantic water that have passed through the N-section, both their average values and their variations. This task is split into two parts: i) what controls the properties of the water approaching the IFR? and ii) how are these properties modified by crossing the ridge?

Thus, we first examine what drives the changes in properties of the water that arrives with the North Atlantic Current at the IFR. It is well known that the temperature and salinity of the Atlantic water flowing towards and across the Greenland-

https://doi.org/10.5194/egusphere-2026-359
Preprint. Discussion started: 29 January 2026

Scotland Ridge are affected by variations of the North Atlantic Subpolar Gyre (SPG) as represented by the Gyre Index (Hátún et al., 2005; Larsen et al., 2012). The original version of the Gyre Index (Häkkinen and Rhines, 2004) was based on Empirical Orthogonal Function (EOF) analysis of satellite altimetry data from a large area in the North Atlantic. Since then, various other versions have been suggested, creating considerable ambiguity (Hátún and Chafik, 2018), and it has been emphasized that one index may not necessarily describe the SPG variation in all regions (Foukal and Lozier, 2017; Biri and Klein, 2019).

Here, we are only concerned with the effect that the SPG has on the properties of the Atlantic water as it approaches the IFR, and we adopt a picture (Foukal and Lozier, 2017) of the SPG as the largest closed cyclonic streamline south of the GSR (Supplementary Fig. S1). To see how changes in this gyre affect the water properties, it is important to know the pathways of the Atlantic water towards the IFR in order to choose the right area for investigations. This question has been addressed before, but there are large variations in the published pathways (e.g., Helland-Hansen and Nansen, 1909; Hansen and Østerhus, 2000; Fratantoni, 2001; Orvik and Niiler, 2002; Larsen et al., 2012; Logemann et al., 2013). Based on the mean dynamic topography and satellite-tracked drifters, we establish the main pathway for the Atlantic water approaching the IFR and perform an EOF analysis in this region to investigate the effects of SPG variations on the Atlantic water flow.

We next examine changes to the water properties as the IF-inflow crosses the IFR. The Atlantic water that crosses the IFR is colder and less saline than the branch flowing through the Faroe-Shetland Channel, and it is further freshened and cooled on its way across the IFR and towards the N-section. This has already been investigated by Larsen et al. (2012) who found that the water freshens by 0.05 psu and cools by 0.7 °C while crossing the ridge. Their study, however, focused on the changes in the maximum salinity core of Atlantic water from the Faroe Bank Channel to the N-section (Fig. 1).

In the present study, we investigate not the changes in the properties of the core of the flow, but rather for the total Atlantic water crossing the IFR from the upstream region on both the Faroese and Icelandic sides in the Iceland Basin to transport-weighted values at the N-section. Our results show stronger cooling and much more freshening than the Larsen et al. (2012) study and we try to identify the processes responsible for these modifications.

2. Materials

2.1. Satellite-tracked drifter data

Satellite-tracked drifter data from the Global Drifter Program were obtained from NOAA (https://erddap.aoml.noaa.gov/gdp/erddap/tabledap/drifter_6hour_qc.html, last access: 14 January 2026). The drifter data are from buoys having a drogue centered at 15 m depth representing the surface flow. We selected quality controlled 6-hourly interpolated drifting buoy data from the Area 50° N–70° N and 10° E–40° W. All available drifters from 1991 and to March 2024 with the drogue attached are used, adding up to 1533 drifters in the area.

The temporal distribution of the drifters crossing the IFR shows substantial gaps in coverage throughout the sampling period from 1991 to 2024. The data is heavily weighted toward the recent period, with 74 drifters crossing the IFR from 2015 to 2024 and only 7 drifters crossing the IFR from 2000 to 2014.

https://doi.org/10.5194/egusphere-2026-359
Preprint. Discussion started: 29 January 2026

2.2. Temperature and salinity data

Hydrographic data from the northern Iceland Basin and the IFR region are analysed. The hydrographic observations were carried out by the Faroe Marine Research Institute (FAMRI) in the years from 1976 to 2024. Data from two standard hydrographic stations located southwest of the IFR are also used. Station I, occupied by the Icelandic Marine and Freshwater Research Institute (IMFRI), is the deepest station on the "Stokksnes" section (ST5). Station V, occupied by FAMRI, is the deepest station on the "V-section" (V06), crossing the Faroe Bank Channel. Northeast of the IFR, we use hydrographic data from two standard sections. These are the 14 standard stations, N01 to N14, on the N-section occupied by FAMRI and the 6 standard stations, KR1 to KR6, on the Krossanes section occupied by IMFRI. With two to six occupations per year, all these stations have been occupied more than a hundred times since 1993. The standard stations and sections are shown in Fig. 1. The hydrographic data are reported as Conservative temperature and Absolute salinity following TEOS-10 standards.

2. 3. Data on sea level height

Altimetry data were selected from the global gridded (0.25°x0.25°) sea level anomaly (SLA) field 1993–2022 available from Copernicus Marine Environment Monitoring Service (CMEMS) (http://marine.copernicus.eu): SEALEVEL_GLO_PHY_L4_MY_008_047. We also use gridded values for the Mean Dynamic Topography (MDT) associated with this data set (Mulet et al., 2021).

3 The Atlantic water pathway towards the IFR

3.1 The Mean Dynamic Topography southwest of the IFR

In the geostrophic approximation, surface velocity is parallel to sea level height (SLH). Data on SLH can thus inform us on the mean surface flow of the water approaching the IFR as well as its variation. The time average SLH – termed the Mean Dynamic Topography (MDT) – is shown in Fig. 2. The background colours indicate the MDT. To the extent that this version of the MDT represents mean flow, the surface water that ends up crossing the IFR flows between the two thick white dashed lines on average. To enhance visibility, the area between these two lines has been overlain by a semi-transparent grey surface, and there is a drop in SLH of 10 cm across it.

The area south of the southern dashed line also has a net north-eastward flow but this water is on its way to pass south and then east of the Faroes rather than north of the Faroes. The curved white arrow close to the western border of Fig. 2 shows water that has entered the eastern Iceland Basin, but is returning towards the west. It has been labelled SPG to indicate that most of this water is part of a closed circulation cell south of the Greenland-Scotland Ridge, which we term the Sub Polar Gyre.

https://doi.org/10.5194/egusphere-2026-359
Preprint. Discussion started: 29 January 2026

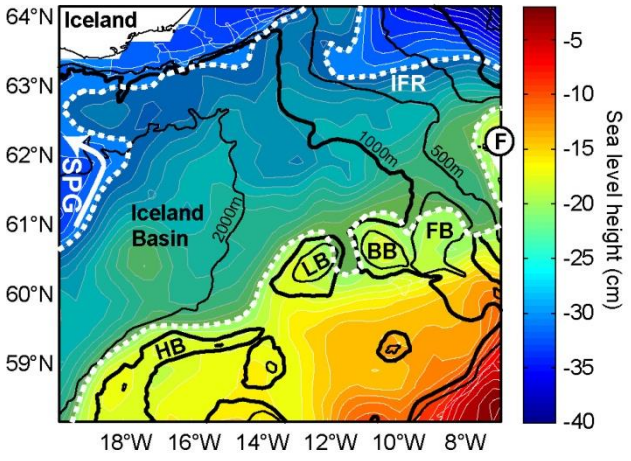

Figure 2. The Mean Dynamic Topography in the region west and southwest of the IFR. The semi-transparent grey region bounded by thick dashed white curves indicates surface water on its way to cross the IFR. The curved white arrow shows intrusion of water from the SPG into the region. Black lines show bottom contours for 500 m, 1000 m and 2000 m with the 1000 m contour thicker. The Faroes are indicated by an "F" in a circle. IFR: Iceland-Faroe Ridge. HB: Hatton Bank. LB: Lousy Bank. BB: Bill Baileys Bank. FB: Faroe Bank.

According to the MDT (Fig. 2), all the water crossing the IFR at the surface has passed through the Iceland Basin on average. Its northward extent is limited by the South Icelandic slope and its southward extent by the plateau and banks west of the Faroes. The accuracy of the MDT is limited by the accuracy of the geoid, altimetry and other input data (Mulet et al., 2021), but Koman et al. (2022) found good correspondence between surface velocities in the Iceland Basin determined from Argo floats and altimetry (their Fig. 6). As will be shown, this water is highly barotropic in the upper 500 m. We therefore expect the surface boundaries in Fig. 2 also to apply to this layer to a high degree.

The barotropic character of the flow also allows a consistency check: Assuming geostrophy, a barotropic flow over a flat bottom at depth D has a volume transport $Q = g{\cdot}\Delta h{\cdot}D{\cdot}f^{1}$, where g is the acceleration of gravity, f the Coriolis parameter and Δh is the sea level difference across the flow. From Fig. 2, Δh is 10 cm. Using the sill depth of the IFR: D = 500 m, Q is found to be 3.8 Sv, which is equal to the observed value (Hansen et al., 2023). The close agreement between the values shows that we should expect a sea level difference across the flow around 10 cm, which provides support for Fig. 2.

3.2 Drifter flow paths towards the IFR

Of the available drifter data, 101 drifters crossed the IFR eastwards from the Iceland Basin to the Norwegian Sea. The IFR is here defined as the area between the 1000 m isobath in the Iceland Basin (the western boundary, WB) and the 500 m isobath in the Norwegian Sea (the eastern boundary, EB). Drifters crossing IFR have crossed these two boundaries, which are extended towards Iceland and Faroes (Fig. 3a). Additionally, there were 44 drifters passing southeast of Faroes into the Nordic Seas (Fig. 3b). Some drifters have crossed the IFR, subsequently turning into the Faroe-Shetland Channel, some even traveling around the Faroe Islands, before turning to the Norwegian Sea. They are only included in Fig. 3a.

https://doi.org/10.5194/egusphere-2026-359
Preprint. Discussion started: 29 January 2026

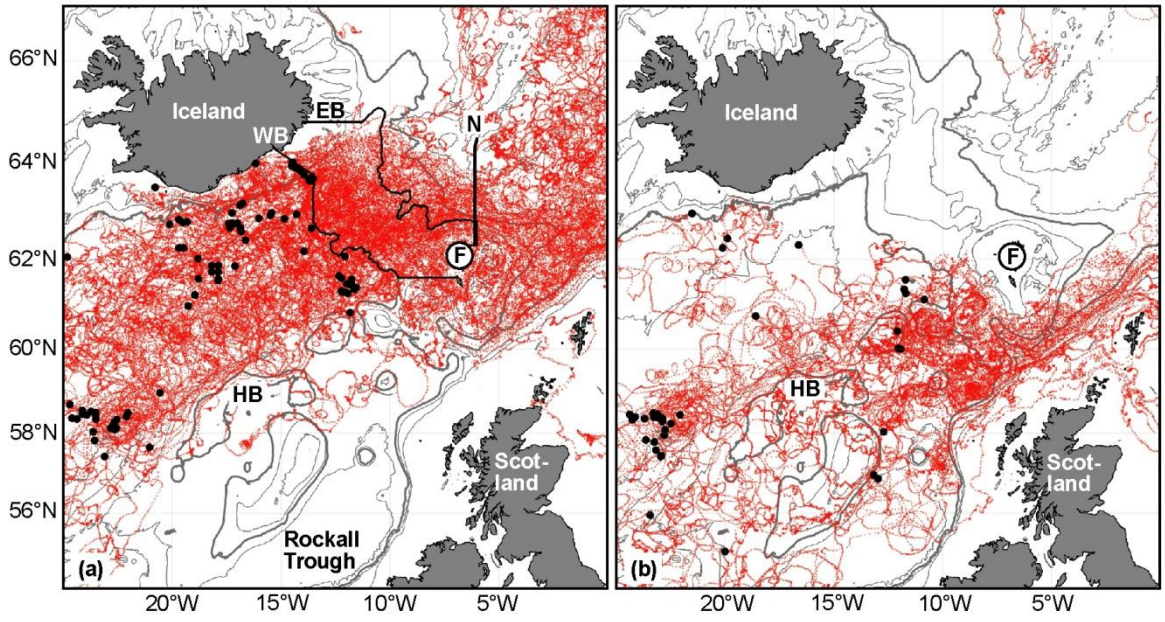

Figure 3. (a) Flow paths of 101 drifters crossing the IFR. Black curves show the western boundary (WB) and the eastern boundary (EB) defining the IFR area. The thick black line north of the Faroes (F) indicates the N-section. **(b)** 44 drifters passing southeast of the Faroes. Black circles on both maps show where the drifters were deployed if they fall inside the map area. Grey lines show bottom contours for 200 m, 500 m, 1000 m, 1500 m, 2000 m and 3000 m with the 1000 m contour thicker. "HB" is Hatton Bank.

The drifter data supports that the origin of the Atlantic Water crossing the IFR into the Norwegian Sea is from the Iceland Basin and it also indicates, that there is little exchange northwestward from the Rockall Trough area across the banks to the Iceland Basin in the surface layer. None of the 101 drifters passing IFR has entered through the western part of the Rockall Trough, although there are eight drifters that flow from the Iceland Basin on to the banks in this area and back to the Iceland Basin and eventually cross the IFR (Fig. 3a and Supplementary Fig. S2). There is exchange of surface water the other way, from the Iceland Basin to the Rockall Trough, as is seen in Fig. 3b.

The drifter dataset is not ideal due to the fact that the drifters were not deployed homogeneously and they will be affected by the wind despite only drifters with the 15 m drogue attached were used (Brambilla and Talley, 2006; Poulain et al., 2009). Westerlies dominate the area and this implies that the Ekman drift on the surface drifters is towards the south. We cannot exclude the possibility that Ekman drift has prevented drifters to pass from the Rockall Trough to the IFR. The southward forcing is however not so strong that it prevents most drifters coming through the Iceland Basin to cross the Iceland-Scotland Ridge between Iceland and the Faroe Islands.

Both the MDT and the drifter data, thus, point at the Iceland Basin as the typical pathway for Atlantic water to approach the IFR. Occasionally, water that has entered the region through the Rockall Trough may perhaps cross the IFR, but the drifter data show that this does not occur frequently. We note that the surface temperature distribution in Fig. 1 also is consistent with the flow field in Fig. 2. These results also agree with a study using vessel-mounted ADCP data from four different routes between Scotland, Iceland and Greenland (Childers et al., 2015) and an earlier drifter study (Jakobsen et al., 2003).

https://doi.org/10.5194/egusphere-2026-359
Preprint. Discussion started: 29 January 2026

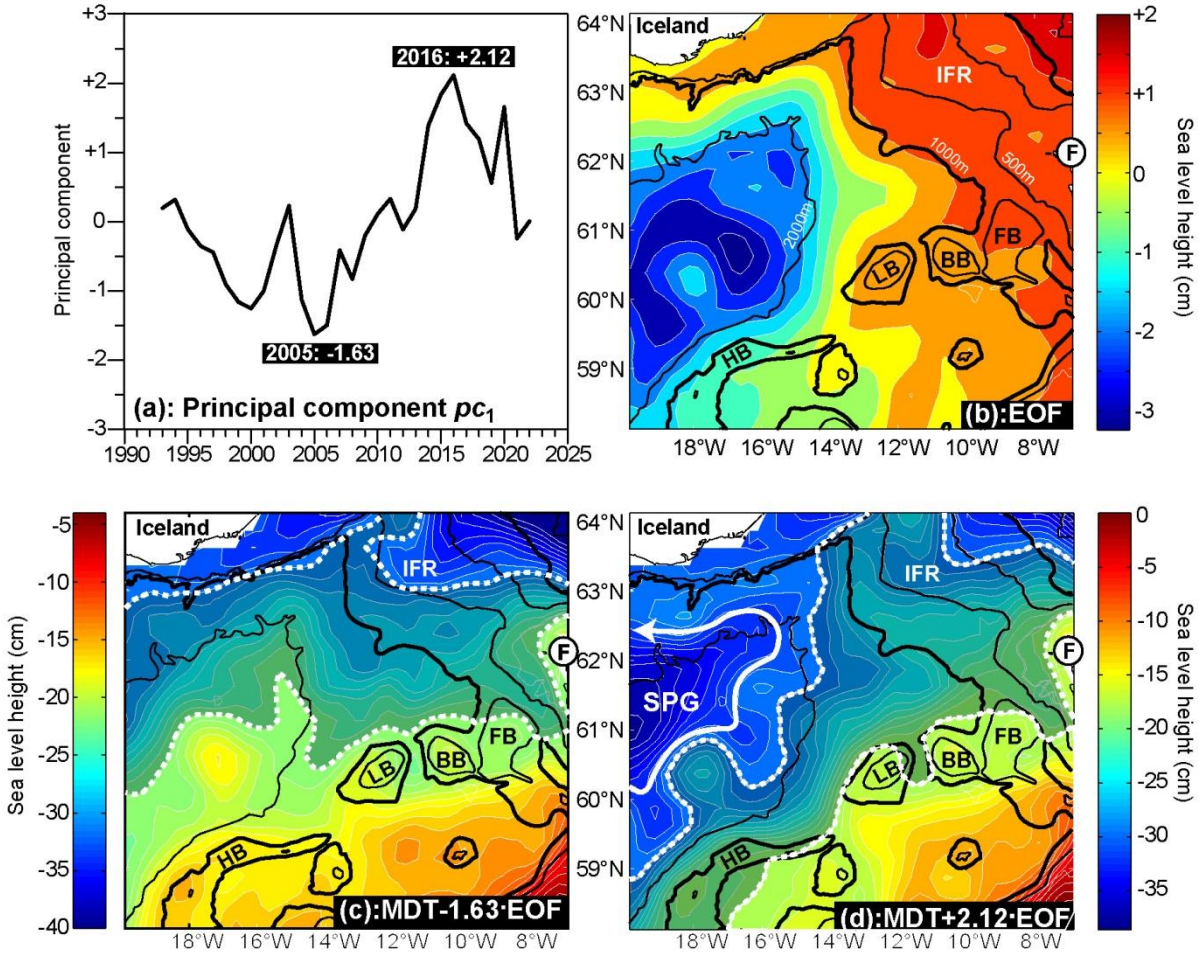

Figure 4. EOF-analysis of annually averaged "modified" (see text) SLA for the 1993–2022 period. **(a)** Principal component (temporal variation) of the first EOF-mode. **(b)** Spatial structure of the first EOF-mode. **(c)** The background colours show the Mean Dynamic Topography added to the first EOF-mode multiplied by -1.63. **(d)** The background colours show the Mean Dynamic Topography added to the first EOF-mode multiplied by 2.12. The semi-transparent grey regions bounded by thick dashed white curves in (c) and (d) indicate surface water on its way to cross the Iceland-Faroe Ridge. The curved white arrow in (d) shows intrusion of water from the SPG into the region. Black lines on the maps show bottom contours for 500 m, 1000 m and 2000 m with the 1000 m contours thicker. The Faroes are indicated by an "F" in a circle. IFR: Iceland-Faroe Ridge. HB: Hatton Bank. LB: Lousy Bank. BB: Bill Baileys Bank. FB: Faroe Bank.

3.3 Inter-annual variations of the surface flow southwest of the IFR

To study the low-frequency circulation changes in the eastern Iceland Basin and the northern parts of the Rockall-Hatton Plateau, an EOF analysis is made on the annually averaged "modified" SLA data for the 1993–2022 period. The "modification" involves subtraction of the spatial average from all grid points at every time-step to remove trends and focus on the local sea level slope which is proportional to sea surface speed in the geostrophic approximation.

For annually averaged modified SLA data, the first EOF mode (Fig. 4a,b) explains more than half (52 %) of the total variance with the second mode only explaining 10 % of the variance. The principal component of the first mode, pc_1, (Fig. 4a)

https://doi.org/10.5194/egusphere-2026-359
Preprint. Discussion started: 29 January 2026

ranges between –1.63 in 2005 and +2.12 in 2016. To illustrate the effect of this variation, the two bottom panels in Fig. 4 show the total flow field (the Absolute Dynamic Topography) when the MDT is added to the spatial EOF-mode multiplied by the principal component at its minimum (Fig. 4c) and its maximum (Fig. 4d) values, respectively.

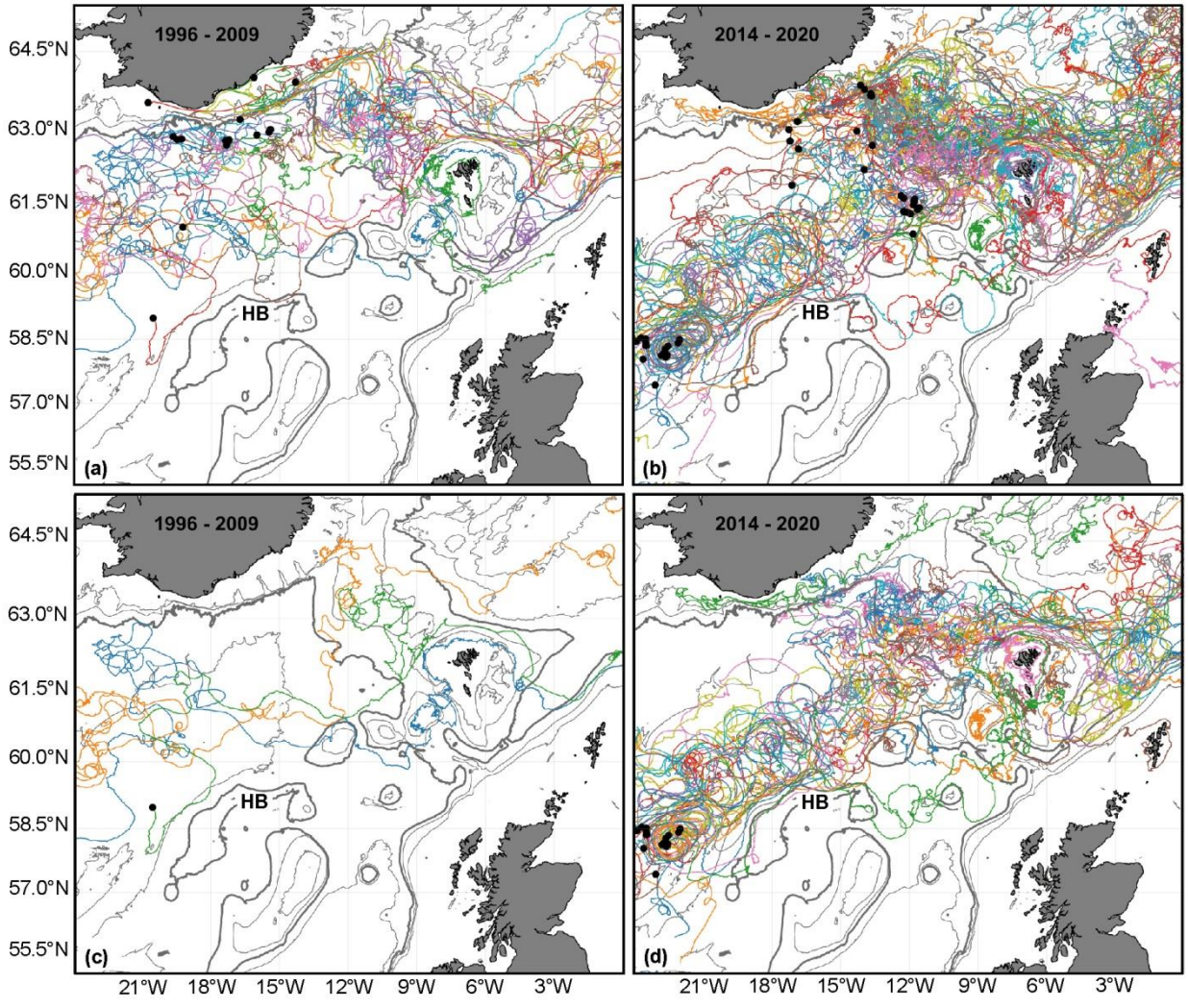

Figure 5 (a), (c) Drifters crossing IFR in a period with no or little intrusion of the SPG into the Iceland Basin (pc_1 was low). **(b), (d)** Drifters crossing IFR in a period where SPG intruded far into the Iceland Basin (pc_1 was high). **(a)** All the drifters (19) crossing in the period from 1996 to 2009. **(c)** The same as in (a), but only those drifters (3) that were deployed south of 60° N. **(b)** All drifters (50) crossing in the period from 2014 to 2020. **(d)** The same as in (b), but only drifters (23) deployed south of 60° N. Black circles show where the drifters were deployed if they fall inside the map area. Grey lines show bottom contours for 200 m, 500 m, 1000 m and 2000 m with the 1000 m contour thicker. HB: Hatton Bank.

From Fig. 4, it appears that the principal component of the first EOF mode, pc_1, is an indicator for the intrusion of the SPG into the eastern Iceland Basin along with a south-eastward migration and focussing of the flow corridor feeding the IFR with Atlantic Water. When pc_1 is at its minimum (Fig. 4c), the traces of SPG, seen in the MDT (Fig. 2), have moved westwards

https://doi.org/10.5194/egusphere-2026-359
Preprint. Discussion started: 29 January 2026

out of the region. The Atlantic water flows through the northern part of the Iceland Basin. When pc_1 is at its maximum, in contrast, the SPG intrudes almost all the way to the IFR (Fig. 4d), and the Atlantic water flow corridor is pushed south-eastwards so that it passes over Hatton Bank. This interpretation is supported by considering the average sea level height (the Absolute Dynamic Topography, ADT) for the two extreme years 2005 and 2016 (Supplementary Fig. S3).

Dividing drifters that cross the IFR into two periods, 1996–2009 with low pc_1 (19 drifters) and 2014–2020 with high pc_1 (50 drifters), we find that the pathway towards the IFR is more southeasterly during the period with high pc_1 than during the period with low pc_1, which is in line with the EOF analysis (Fig. 5a,b). In Fig. 5c and d, only drifters deployed south of 60° N are included. This ensures that our conclusion avoids being an artefact of the potentially inhomogeneous deployment of the drifters in the two periods. We observe that drifters in the period with high pc_1 (2014–2020, 23 drifters) do not enter the northwestern part of the Iceland Basin, which is in agreement with Fig. 4d. In contrast, during the period with low pc_1 (1996–2009), although only 3 drifters are available for this period, two out of three drifters enter this area, which is consistent with Fig. 4c.

4 Long-term variations of the Atlantic water properties

4.1 Water mass properties upstream and downstream of the IFR

Mean profiles for the two standard stations I and V southwest of the IFR (locations are shown in Fig. 1) are fairly barotropic except for the seasonal surface layer and below around 400 m in the Faroe Bank Channel (station V), where cold overflow water is under the Atlantic water (Fig. 6a,b).

To characterize the water mass variations of the Atlantic water approaching the IFR region, we compute depth-averaged temperature and salinity over the upper 500 m, corresponding to the approximate sill depth of the IFR. Although typically more frequent, there are years with only two occupations at different times of the year for both station I and V. The time series have been de-seasoned using the same method as in Larsen et al. (2012), but annual averages will still be rather uncertain. To reduce this uncertainty, the time series plotted in Fig. 6c,d have therefore been averaged over three years (running mean).

Although the values at station V (cyan curves) and station I (orange curves) at a specific time typically differ for both temperature (Fig. 6c) and salinity (Fig. 6d), these differences are relatively small compared to the overall variations throughout the period. This motivates the generation of time series for “Iceland Basin temperature”, T_{IB}, and “Iceland Basin salinity”, S_{IB}, by averaging the 3-year running mean values at stations I and V. Water approaching the central parts of the ridge, away from both I and V, are expected to have properties intermediate between I and V in the upper parts. Below around 400 m, both temperature and salinity of this water will be less reduced by Faroe Bank Channel overflow than at station V. The time series T_{IB} and S_{IB}, thus, will not represent the average properties of the Atlantic water impinging on the IFR exactly, but they are not likely to be overestimates. In the following, they will be used to represent upstream values for the temperature and salinity of the Atlantic water reaching the IFR.

https://doi.org/10.5194/egusphere-2026-359
Preprint. Discussion started: 29 January 2026

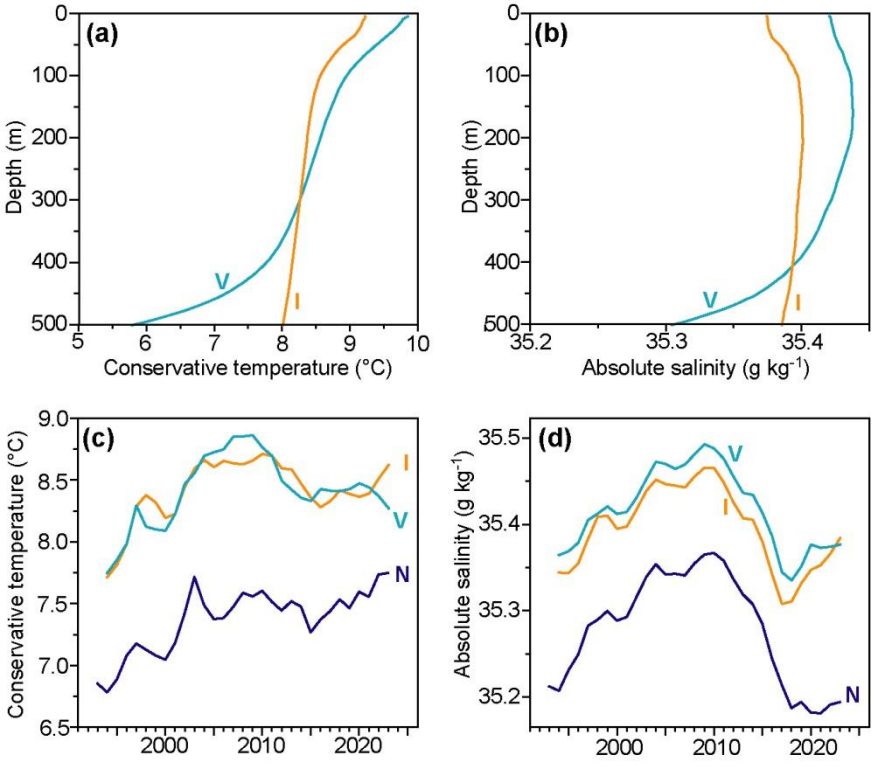

Figure 6. Mean temperature **(a)** and salinity **(b)** profiles for the two standard stations I (orange) and V (cyan) upstream of the IFR. For positions see Fig. 1. Three-year running mean de-seasoned temperature **(c)** and salinity **(d)** averaged from the surface to 500 m depth for the two standard stations I (orange) and V (cyan). Dark blue curves show transport-weighted temperature **(c)** and salinity **(d)** on the N-section based on Hansen et al. (2023).

The properties downstream of the ridge are monitored at the N-section (location shown in Fig. 1). Average water mass characteristics on the N-section are shown in Fig. 7. The position and properties of the core are variable and unlike the stations upstream of the IFR (I and V), the water column at the N-section is highly variable vertically as well as horizontally. Therefore, it is not possible to use a simple depth average for a few standard stations to show the Atlantic water properties at this section. Instead transport-weighted temperature and salinity are used. Annually averaged values (1993–2023) for transport-weighted temperature and salinity on the N-section updated from Hansen et al. (2023) are compared to the standard stations upstream of the IFR (Fig. 6c,d).

On inter-annual time scales, there is little similarity between the properties upstream of the IFR, T_{IB} and S_{IB}, and the downstream properties as monitored on the N-section. On longer time scales, however, the variations upstream and downstream exhibit considerable similarity. During the IFR-crossing, the Atlantic water has been cooled and freshened, but by relatively stable amounts. Thus, the long-term variations of both temperature and salinity of the IF-inflow at the N-section are primarily caused by processes upstream of the IFR.

https://doi.org/10.5194/egusphere-2026-359
Preprint. Discussion started: 29 January 2026

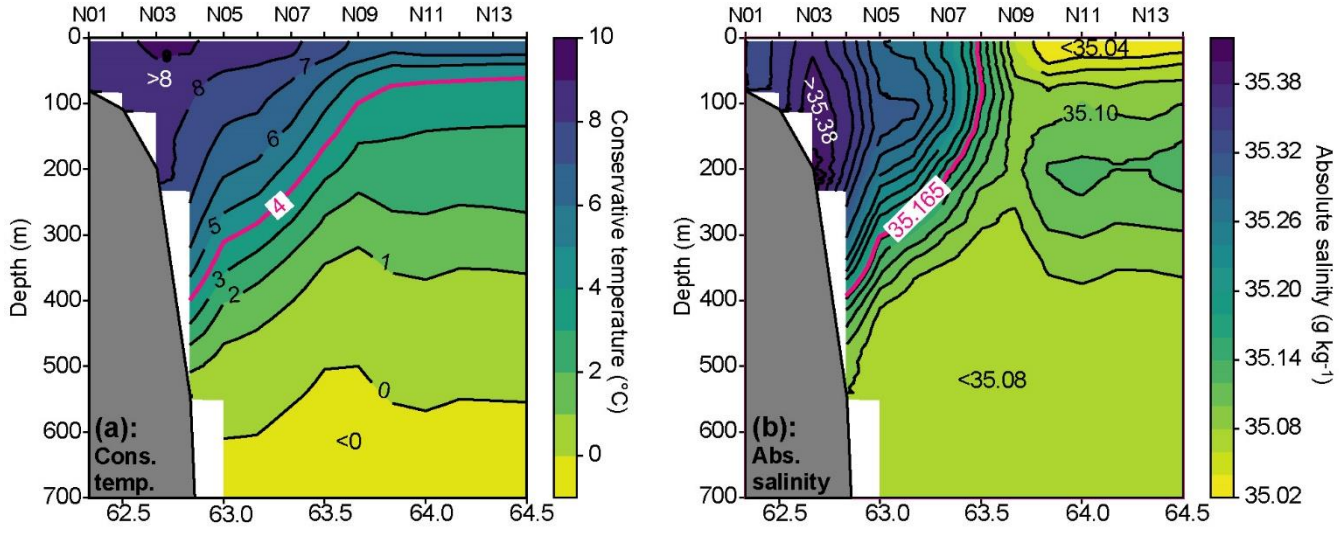

Figure 7. Average water mass characteristic at the N-section. Mean Conservative temperature **(a)** and Absolute salinity **(b)** for the period from 1993 to May 2024 from 99 cruises where all 14 standard stations were occupied. Magenta lines show the 4 °C isotherm and the 35.165 g kg^{-1} isohaline (corresponding to the 35.0 isohaline in practical salinity units), used by Hansen et al. (2023) to define the deep and northern boundary of Atlantic water on the section.

4.2 Causes of the long-term variations

In Fig. 8a, time series of Iceland Basin temperature, T_{IB}, and salinity, S_{IB}, are plotted together with the principal component, pc_1 (Fig. 4a), of the first (modified) sea level EOF mode (plotted on an inverted scale). For salinity, the similarity between the cyan and the black curves in Fig. 8a suggests an influence on S_{IB} from the SPG although with a delay. Such a link has previously been suggested for the early part of the time series through a large-scale Gyre Index (Hátún et al., 2005; Larsen et al., 2012). With the more recent ambiguity of this index (Hátún and Chafik, 2018) and its regional variation (Biri and Klein, 2019), we decided instead to focus on a regional rather than a large-scale part of the SPG. For that reason, the EOF analysis in Fig. 4 was restricted to a small region around the Iceland Basin, so that unrelated variations would not disrupt the signal.

The principal component, pc_1, of the first EOF mode is therefore not an index for the SPG as a whole. Rather it represents the intrusion of cold low-salinity SPG-water into the Iceland Basin, which provides a causal foundation for the relationship between salinity (cyan curve) and pc_1 (black curve) in Fig. 8a. For temperature, the correspondence between pc_1 and T_{IB} in Fig. 8a is not as clear, especially for the period after 2010. This is also the period when the variations of T_{IB} and S_{IB} in Fig. 8a start to diverge. Before that, the two parameters tended to co-vary as noted by Larsen et al. (2012). After 2010, when pc_1 became strongly positive, only salinity seems to have responded to this SPG intrusion, whereas temperature remained almost constant.

https://doi.org/10.5194/egusphere-2026-359
Preprint. Discussion started: 29 January 2026

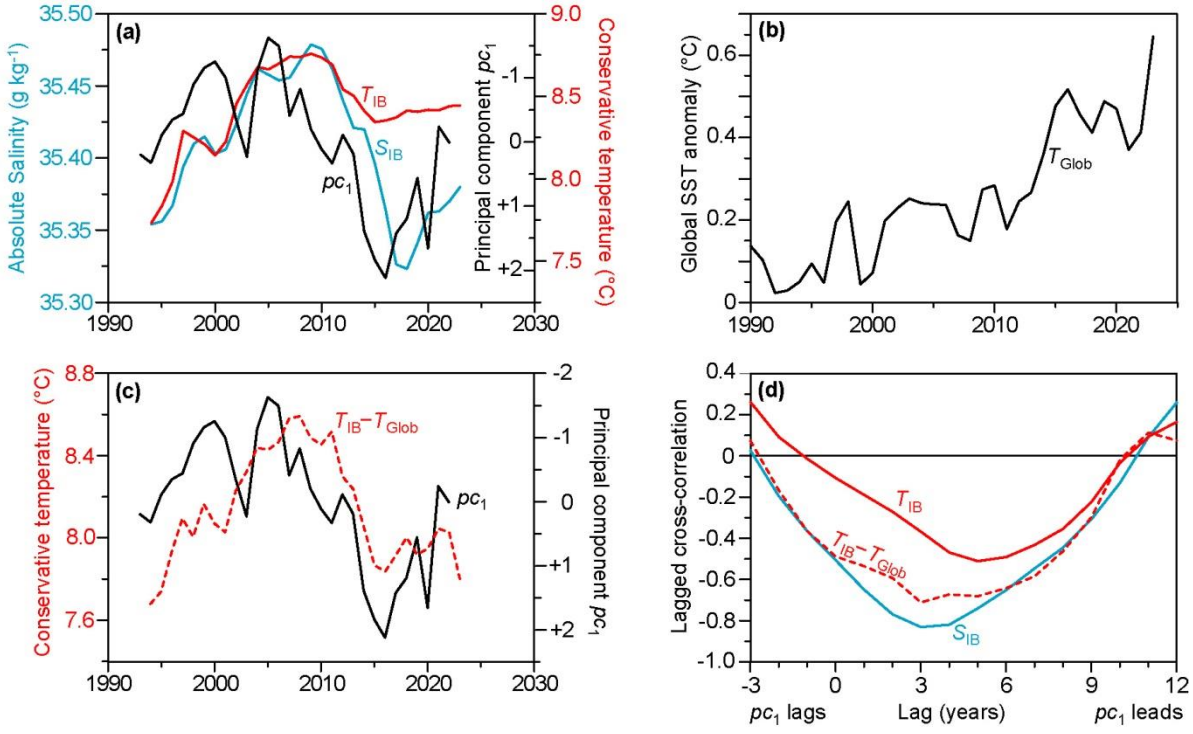

Figure 8. (a) Three-year running mean Absolute salinity S_{IB} (cyan curve) and Conservative temperature T_{IB} (red curve) of the 500 m layer of Atlantic water just before reaching the IFR together with the principal component pc_1 from Fig. 4a (black curve, note inverted scale). **(b)** The global sea surface temperature anomaly T_{Glob} (deviation from the 1971–2000 average) downloaded from NOAA (www.epa.gov/climate-indicators/climate-change-indicators-sea-surface-temperature). **(c)** $T_{IB} - T_{Glob}$ (dashed red curve) together with pc_1 (black curve, note inverted scale). **(d)** Lagged cross-correlation between pc_1 and S_{IB} (cyan curve), between pc_1 and T_{IB} (continuous red curve) and between pc_1 and $T_{IB} - T_{Glob}$ (dashed red curve).

This indicates the occurrence of some other process counteracting the effects of SPG intrusion for temperature, but less for salinity. The obvious candidate for this process is global warming, which especially has affected sea surface temperature (SST) after 2010 (Fig. 8b). To test this hypothesis, we subtract an estimate of the global SST anomaly, labelled T_{Glob}, from T_{IB} and this time series, $T_{IB} - T_{Glob}$, (dashed red curve in Fig. 8c) provides a considerably better fit to pc_1 than T_{IB}. Whereas salinity seems mainly to be a delayed response to SPG intrusion, this indicates that temperature is better explained as a combination of SPG intrusion and global warming.

Using the global SST anomaly as an indicator for the effect of global warming on the 0–500 m depth layer southwest of the IFR can only be considered a rough approximation. A more local indicator would have been preferable, but the more local the parameter we choose, the more we risk the fallacy of circular reasoning by using local temperature to explain local temperature. The parameter $T_{IB} - T_{Glob}$, thus, is only a rough indicator of Iceland Basin temperature without the effect of global warming. Nevertheless, the fit between pc_1 and $T_{IB} - T_{Glob}$ in Fig. 8c appears to be considerably better than the fit between pc_1 and T_{IB} in Fig. 8a. This is confirmed in Fig. 8d, which shows that the best correlation between pc_1 and $T_{IB} - T_{Glob}$ is for the

https://doi.org/10.5194/egusphere-2026-359
Preprint. Discussion started: 29 January 2026

same lag, 3 years, as the best correlation between pc_1 and S_{IB}. For this lag, SPG intrusion explains 69 % of the variance in S_{IB} and 51 % of the variance in $T_{IB} - T_{Glob}$. Attaching statistical significance to these statements is made problematic by the high degree of serial correlation, which typically reduces the number of degrees of freedom to 5 or less.

Most of the salinity variations of the Atlantic water approaching the IFR may therefore be seen as a 3-year delayed response to the intrusion of SPG-water into the Iceland Basin. For the temperature variations, the same applies, except that we have to add the global warming. A delay in the temperature and salinity responses to SPG variations was to be expected since the water is being modified throughout its path along the boundaries of the two gyres and studies on anomaly propagation in the North Atlantic (e.g., Sutton and Allen, 1997; Årthun et al., 2017) suggest that three years may be appropriate. In years when *pc1* is high and the SPG extends far eastwards in the Iceland Basin (Fig. 4d), a smaller lag might be expected and Fig. 8 indicates that this may well be the case.

5 Water mass modification during IFR-crossing

5.1 Observed cooling and freshening during the crossing

From Fig. 6, it is clear that the Atlantic water crossing the N-section has been strongly cooled and freshened relative to the water approaching the ridge from the Iceland Basin. Averaged over the period 1993–2023 the cooling is at least 1 °C and the freshening at least 0.1 g kg^{-1} (Table 1).

Table 1. Averages for the period 1993–2023 of transport-weighted properties on the N-section and of 1–500 m depth-averaged properties on stations "I" and "V" (time series shown in Fig. 6c,d). The last two columns list differences.

	N-sect (Tr-w)	"V" (0–500m)	"I" (0–500m)	"V" minus N	"I" minus N
Conservative temperature (°C)	7.37	8.40	8.40	1.03	1.03
Absolute Salinity (g kg^{-1})	35.28	35.42	35.39	0.14	0.11

Table 1 indicates more cooling and much more freshening than was reported by Larsen et al. (2012) who reported a cooling of 0.7 °C and a freshening of 0.05 psu. They, however, studied changes in the core properties, not the total Atlantic water crossing the IFR. Considering the different approach, our result seems plausible compared to theirs.

5.2 Modifications caused by atmospheric forcing

To quantify the contribution of air-sea interactions to the observed temperature and salinity changes of the water mass traversing the IFR, the transit time of the water mass must be determined. To estimate the transit time for the water parcels to cross from the Iceland Basin to the Norwegian Sea, we calculate the crossing times of individual drifters. The crossing time is defined from when a drifter crosses the Western boundary of the ridge (WB) until it crosses the N-section north of the Faroe Islands (Fig. 3a). 97 of the 101 drifters that crossed the IFR, reached the N-section. As many drifters have crossed the WB

https://doi.org/10.5194/egusphere-2026-359
Preprint. Discussion started: 29 January 2026

several times, both minimum and maximum crossing times were calculated. The minimum crossing time was 52 days on average as defined by the last crossing of the WB until the first crossing of the N-section. The maximum crossing time was 75 days on average and spans from the first crossing of the WB until the first crossing of the N-section. The actual mean transit time falls somewhere between these two estimates.

We have used the same method as Larsen et al. (2012) with climatic values for heat flux (55 W m^{-2}) and a net freshwater input over the typical 75 days (maximum) transit time (0.09 m) to estimate the effects of air-sea interactions on temperature and salinity during the ridge crossing. The result is that only ~22 % of the observed cooling and ~8 % of the observed freshening (Table 1) are explained by air-sea interaction.

5.3 Modifications caused by mixing with Arctic water masses

If not caused by atmospheric forcing, mixing with colder and less saline water masses of Arctic origin is the only explanation for the change in the Atlantic Water during the IFR crossing. Overflow of Arctic water across the IFR is a well established process (e.g., Tait, 1967). Some of this water has been produced remotely (e.g., Hansen and Østerhus, 2000), but Arctic water masses also sink in the Iceland-Faroe Front (IFF) and follow the bottom below the Atlantic inflow (Meincke, 1978) or subduct from the surface layer of the IFF and intrude into the Atlantic water (Beaird et al., 2016). Arctic water masses also cross the front in eddies (Hansen and Meincke 1979, de Marez et al., 2025). These processes are responsible for both vertical and horizontal mixing between the water masses. The relative importance of these processes is beyond the scope of this work. We focus on the overall impact of the mixing.

5.3.1 Observed modifications over the IFR

To examine the water mass transformation across the IFR we analyse CTD data from the northeastern Iceland Basin and the IFR region. The CTD profiles were divided into three regions: i) Upstream of the IFR; ii) The western flank of the IFR; iii) The ridge crest of the IFR (Fig. 9a). Mean temperature and salinity profiles for each of these regions are shown in Fig. 9b,c. The difference between the mean temperature and salinity profiles for the three areas is largest at depth and decreasing towards the surface. This indicates that the deepest part of the water column is modified the most. Even though the dataset, from which average profiles for the IFR area are calculated, spans over many locations and a long period of time this is clearly visible. It appears that most of the change has already occurred when the Atlantic water has reached the ridge crest (blue curves in Fig. 9). Standard station N05, which is north of the Atlantic water core on the N-section (Fig. 7), is further modified. In contrast, stations N03 and N04 over the Faroe slope are less modified, indicating a more direct route.

https://doi.org/10.5194/egusphere-2026-359
Preprint. Discussion started: 29 January 2026

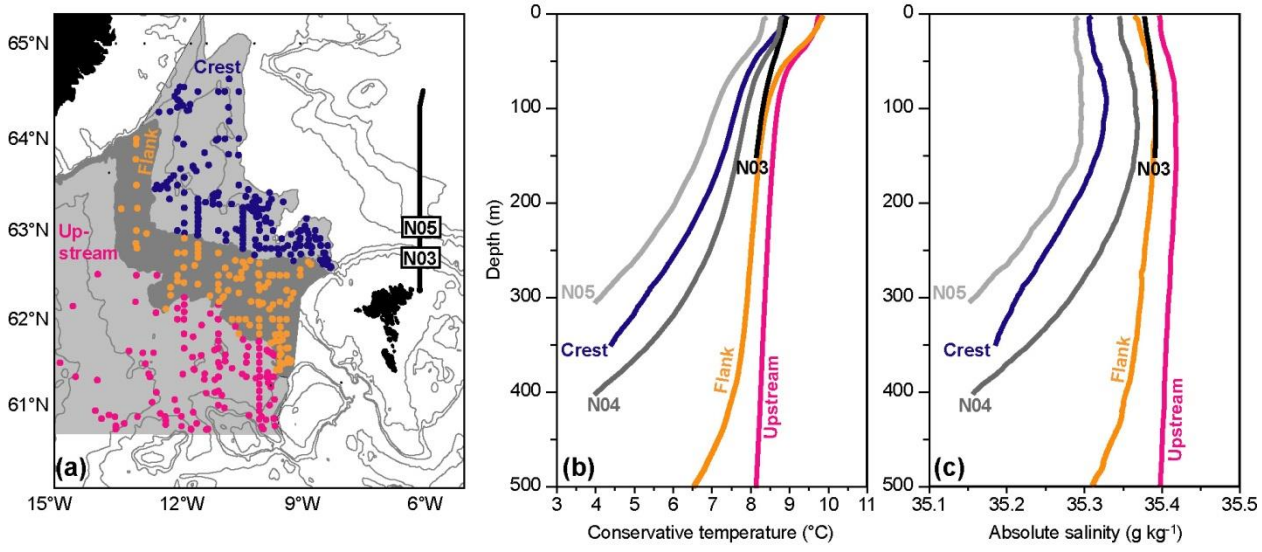

Figure 9. (a) The CTD profiles in the IFR area were divided into three regions: i) Upstream of the IFR (magenta). This region is in the Iceland Basin from 60.7° N and north to the 1000 m isobath and west of 9.6° W. There are 209 CTD casts in this region. ii) The western flank of the IFR (orange). This is from the 1000 m isobath to the 500 m isobath in the Iceland Basin. Here there are 139 CTD casts. iii) The ridge crest (blue). This region is from the 500 m isobath in the Iceland Basin to the 500 m isobath in the Norwegian Sea, with 330 CTD casts. CTD stations are shown with a dot. The area borders are shown with gray shading. The N-section is shown with a thick black line north of the Faroes and two standard CTD stations N03 and N05 are indicated. Thin grey lines show bottom contours for 200 m, 400 m, 500 m, 1000 m, 1500 m, 2000 m and 3000 m. Mean temperature **(b)** and salinity **(c)** profiles for the three regions in (a). Upstream and on the western flank only CTD casts that are at least 500 m deep were included. On the crest, only casts that are at least 350m were included. The profiles for the three standard stations on the N-section N03, N04 and N05 are also shown down to the depth of the 4 °C isotherm, defined as the deep boundary of Atlantic water on the section (Hansen et al., 2023).

5.3.2 Where do the modifications take place?

For mixing in a specific region to affect the water column, the water has to spend sufficient time in the region. This may be investigated by drifter data. To identify spatial clustering in the drifter movements across the IFR, we analysed gridded drifter data. The grid used is 0.1 degrees latitude and 0.2 degrees longitude. Our analyses reveal that the drifters spent a disproportionate amount of time over the western flank of the ridge, as shown in Fig. 10a. However, regions where drifters spend much time do not necessarily indicate high drifter concentration. Such patterns could also reflect low velocity of a few drifters in the area and therefore long periods in these bins. To obtain a more accurate representation of the drifter distribution across the IFR the number of unique drifter ID-numbers in each grid cell is included (Fig. 10b). A large number of unique drifters are observed on the western flank, indicating that the western flank is a common area for drifters to occupy.

Figure 10 confirms that the satellite-tracked drifters that cross the IFR exhibited prolonged residence times on the western flank of the IFR. Together with a high level of eddy kinetic energy (EKE) (Fig. 11), this indicates enhanced mixing in this area and that the Atlantic water spends sufficient time over the western flank for the mixing to act.

https://doi.org/10.5194/egusphere-2026-359
Preprint. Discussion started: 29 January 2026

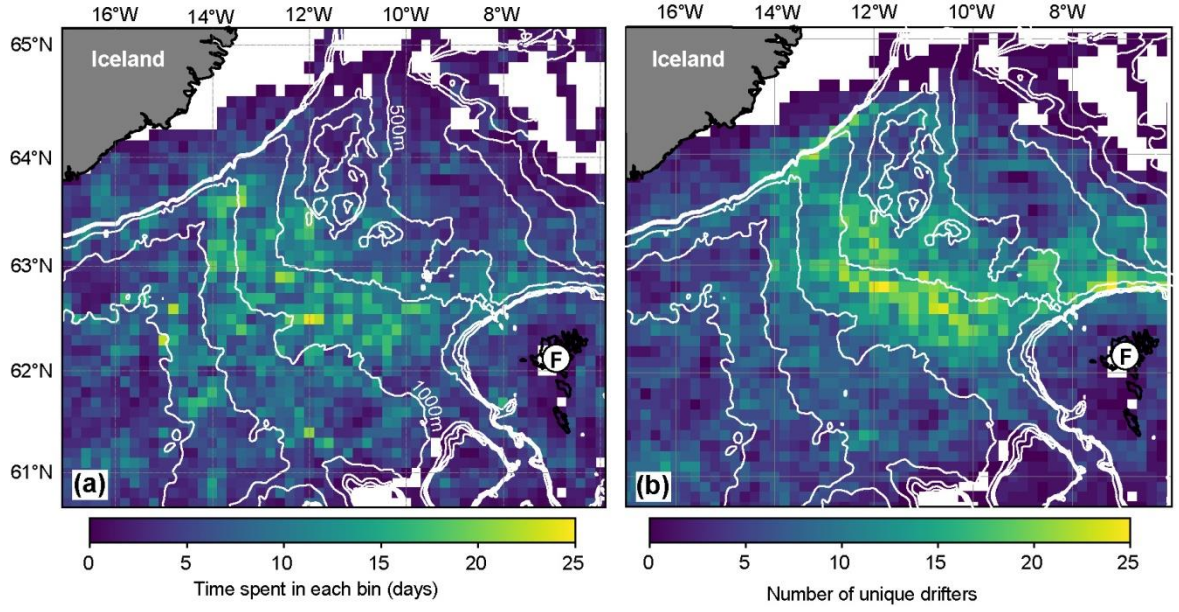

Figure 10. (a) Time spent in each grid cell by the 101 drifters crossing the IFR. **(b)** Number of unique drifter ID numbers in each grid cell. The white lines on both maps show bottom contours for 300m, 350 m, 400 m, 500 m, 1000 m, 1500 and 2000 m. An "F" in a white circle shows the Faroe Islands.

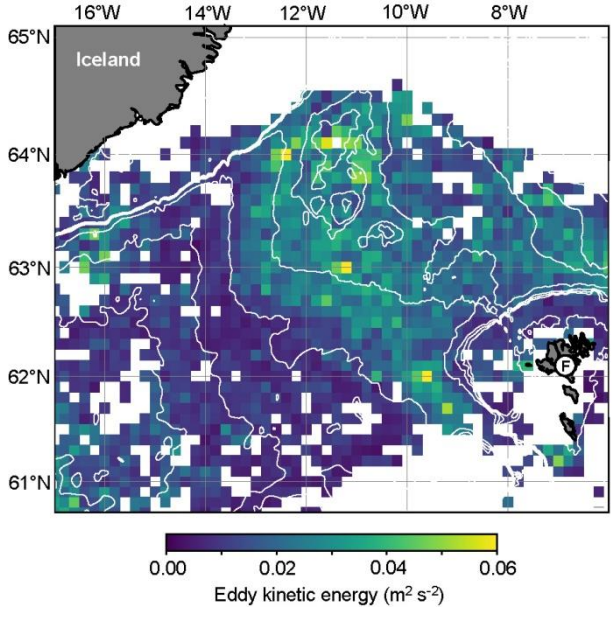

Figure 11. Distribution of the eddy kinetic energy (EKE) calculated from velocities from the same drifter data as in Fig. 10. The EKE is only shown for bins with at least 5 different drifters passing. The white lines show bottom contours for 300m, 350 m, 400 m, 500 m, 1000 m, 1500 and 2000 m. F indicates the Faroe Islands.

https://doi.org/10.5194/egusphere-2026-359
Preprint. Discussion started: 29 January 2026

Figure 9 demonstrates that the Atlantic water changes character from an almost barotropic (depth-independent) water column upstream of the ridge (upper 500 m) to a much more baroclinic water column on and downstream of the ridge. A possible explanation is that the barotropic current requires baroclinicity to cross the ridge. According to the Taylor-Proudman theorem, a barotropic water column is prevented from crossing isobaths under the geostrophic assumption, that is as long as friction can be ignored. Thus, the baroclinicity added by admixture of Arctic water at depth, as the water approaches the IFR, is essential for enabling the crossing. This may also explain why the water spends an extended time over the western flank, as baroclinic development must occur before crossing takes place.

5.3.3 Water masses that are admixed into the Atlantic water

Since most of the mixing occurs over the IFR, some of the cold low-salinity water admixed into the IF-inflow is likely to be the near-bottom water mass that is flowing towards the Iceland Basin on its way to become overflow. Bottom temperature observations have documented that this overflow water is found all along the ridge crest although in variable concentrations (Jochumsen et al., 2016). Over the western flank of the ridge, old (Meincke, 1972) as well as newer (e.g., Beaird et al., 2013; Jochumsen et al., 2016, Supplementary Fig. S4) observations also show high concentrations of overflow water, again with a high variability.

Mixing between the warm, saline Atlantic inflow and the less saline, cold Arctic water masses is likely initiated on the western flank of the IFR, near the inflow-overflow interface. This interface lies close to the bottom on the western flank and ascends across the IFR. Both the initiation of mixing and the ascent of the interface are consistent with the average temperature and salinity profiles (Fig. 9).

Temperature-salinity (T-S) diagrams for the same three regions as in Fig. 9 are presented in Fig. 12. Upstream of the IFR in the Iceland Basin, the upper 500 m consist of warm and saline water of Atlantic origin, labeled “IB” (Fig. 12a). Over the IFR (Fig. 12b,c), the “IB” water has been joined by cold Norwegian Sea Arctic Intermediate Water (NSAIW) from intermediate depths in the Norwegian Sea, which is a clear indicator of overflow.

Between the “IB” and the “NSAIW” waters, there are indications of a third water mass of intermediate temperature and low salinity, which is especially prominent over the ridge crest (Fig. 12c). In Fig. 12, this water mass has been labeled “KR”, which refers to the Icelandic standard section “Krossanes”. The Krossanes section is located east-west at 65° N off the east coast of Iceland (Fig. 1) across the East Icelandic Current carrying the Arctic water that meets the Atlantic water in the Iceland-Faroe front (Perkins et al.,1998). Average water mass characteristics on the Krossanes section are shown in Fig. 13.

https://doi.org/10.5194/egusphere-2026-359
Preprint. Discussion started: 29 January 2026

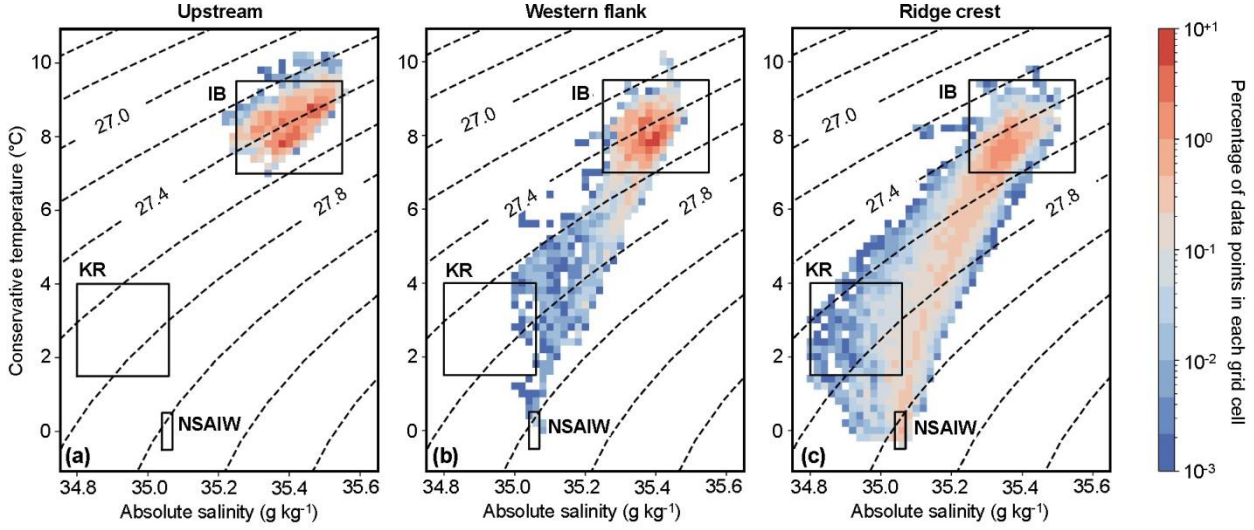

Figure 12. T-S diagrams for the same three regions and the same CTD-profiles as in Fig. 9. **(a)** Upstream of the IFR (100–500 m depth). **(b)** The western flank of the IFR (100–500 m depth). **(c)** The IFR crest (100–350 m depth or bottom). The uppermost 100 m are not shown due to the seasonal thermocline. The ranges of the "IB", "KR" and "NSAIW" are shown with black boxes. The range of "IB" is found from the T-S diagram of the uppermost 500 m at stations V and I (Supplementary Fig. S5a,b). The range of "KR" is found from the T-S diagram of the uppermost 100 m at the Krossanes section, stations KR2–KR6 (Supplementary Fig. S5c). The range for NSAIW is adopted from Hansen and Østerhus (2000) with salinity converted to absolute salinity.

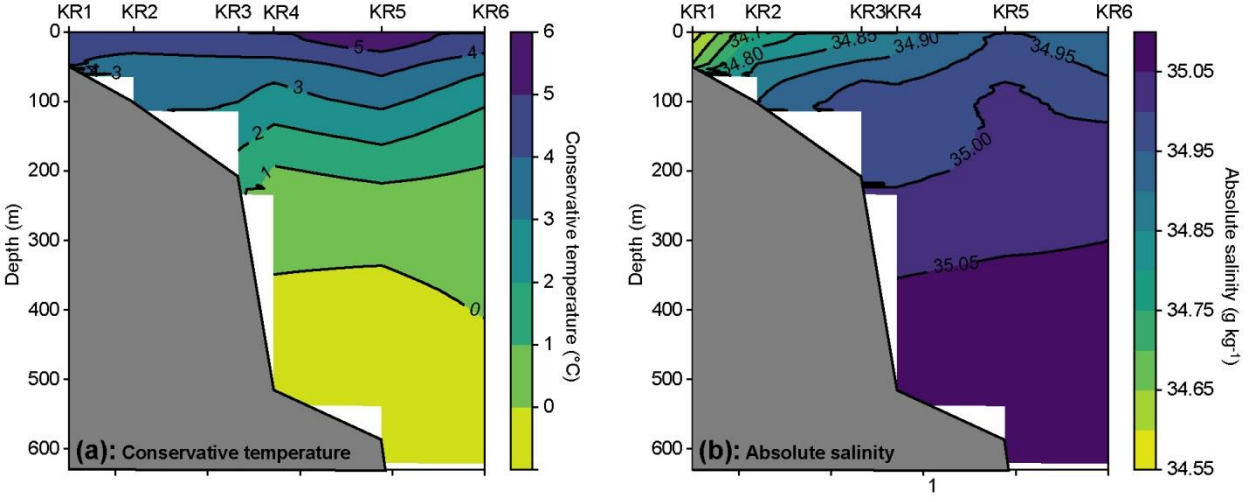

Figure 13. The Krossanes section. Mean temperature (a) and salinity **(b)** for the period from 1993 to May 2024, based on 102 cruises where all 6 standard stations were occupied.

A detailed discussion of source waters and mixing processes is beyond the scope of this study, but we choose to use the 0–100 m depth layer on the Krossanes section for the intermediate low-salinity water mass. The reason for choosing this depth layer is that the Modified East Icelandic Water (MEIW), as described by Read and Pollard (1992), sinks from near-surface layers in the frontal zone. This water mass is formed as a mixture of Atlantic water and low-salinity water brought to the area

https://doi.org/10.5194/egusphere-2026-359
Preprint. Discussion started: 29 January 2026

by the East Icelandic Current. Fogelqvist et al. (2003) showed that the MEIW joins the overflow across the IFR. During this descent, it is modified by mixing and gains density, but remains less dense than the other, deeper sources of overflow water (Read and Pollard, 1992; Fogelqvist et al., 2003). Notably, Fogelqvist et al. (2003) found that MEIW represents most of the overflow across the IFR and is the uppermost overflow water, suggesting that mixing with MEIW is the main mechanism for modifying the Atlantic inflow across the IFR. Also, if deeper layers on the Krossanes section were included, they would more or less fall on the mixing line between the "KR" square and the NSAIW square in Fig. 12.

To a first approximation, it therefore seems likely that the 0–100 m depth layer at KR2–KR6 represents the water mass that is admixed into the IF-inflow, causing it to cool and freshen. To test this hypothesis, we combined annually averaged properties of this water mass with annual averages from the Iceland Basin time series in a ratio of 1:3. For both temperature and salinity, this mixture fits remarkably well with the properties observed at the N-section (Fig. 14).

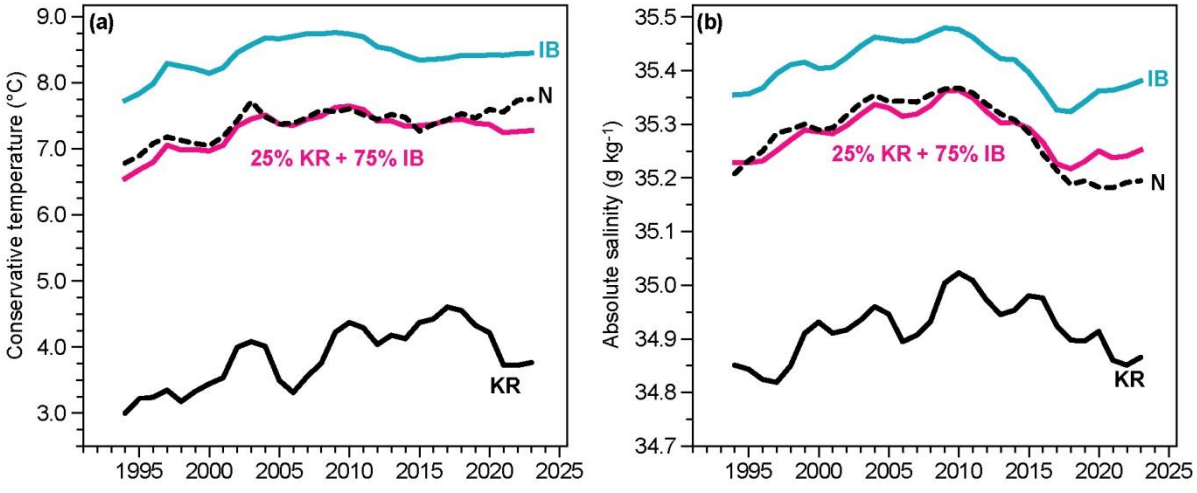

Figure 14. Annual values for temperature **(a)** and salinity **(b).** The continuous black curves are 3-year running mean averages of the water from the surface to 100 m depth for the Krossanes section (KR). The cyan curves show the 3-year running mean averages of the 500 m layer of Atlantic water just before reaching the IFR (IB as in Fig. 8). The dashed black curves show annual values for transport-weighted temperature and salinity on the N-section updated from Hansen et al. (2023) (N as in Fig. 6c,d). The magenta curves are the result when combining the Krossanes series (black) with the Iceland Basin series (cyan) in a 1 to 3 ratio.

On decadal time scales, the variations of the transport-weighted properties of the water that has crossed the ridge (dashed black curves in Fig. 14) are similar to the variations upstream of the ridge (cyan curves). This suggests that the processes modifying the Atlantic water across the IFR are relatively constant since the cooling and freshening of the IF-inflow across the IFR are fairly stable throughout the whole period from 1993 to 2023, except for the last few years. This divergence started after the rapid water mass changes in the Iceland Basin around 2015 (Fig. 8 and Holliday et al., 2020). Choosing a 0–200 m depth interval on the Krossanes section gives the same good fit, but a slightly different mixing ratio (not shown).

https://doi.org/10.5194/egusphere-2026-359
Preprint. Discussion started: 29 January 2026

6 Transport through the N-section

The time series of the annually averaged volume transport and heat transport relative to 0 °C carried by the IF-inflow through the N-section presented in Hansen et al. (2023) were extended two years (Fig. 15 and Table 2). From 1993 to 2023, the volume transport of the IF-inflow increased by (12±7) %, while the heat transport relative to 0 °C increased by (16±8) %. Compared to the former time series (Hansen at al., 2023) the trends are now higher and more significant in the extended time series. The change compared to the average value is higher for relative heat transport due to the fact that the temperature (Fig. 6c) as well as the volume transport has increased.

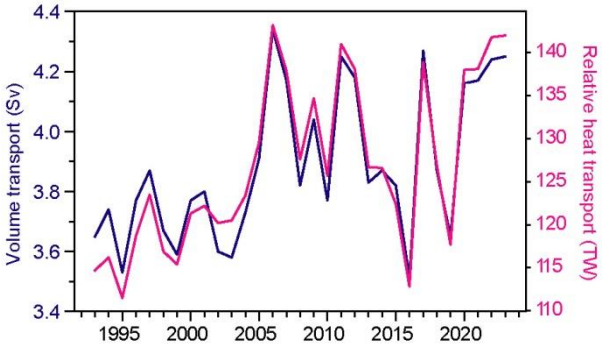

Figure 15. Annually averaged volume transport (blue) and relative heat transport (magenta) across the N-section. The heat transport is relative to a temperature of 0 °C. Updated from Hansen et al. (2023).

Table 2. Characteristics of the two transport time series of IF-inflow through the N-section (Fig. 15). Uncertainty estimates for the average values are based on Hansen et al. (2015). The trends are listed with 95 % confidence intervals. "Change" indicates the relative (to average) change through the 1993–2023 period.

Time Series	Average	Trend	p-value	Change
Volume transport	(3.9 ±0.5) Sv	(0.015 ± 0.009) Sv yr^{-1}	0.002	+(12±7) %
Heat transport relative to 0 °C	(127±15) TW	(0.67 ± 0.32) TW yr^{-1}	0.0002	+(16±8) %

The IF-inflow is part of the northernmost limb of the AMOC but rather than weakening, as projected for the AMOC at lower latitudes, it has been strengthening. This is consistent with some model simulations, which suggest a transient increase of deep-water formation due to "Atlantification" of the northern parts of the Arctic Mediterranean (Bretones et al., 2022). When the sea ice melts, the ocean comes into direct contact with the air and is cooled, enhancing deep-water formation. The result is that even though ventilation decreases in the Nordic Seas, it is strengthened in the Barents Sea and the Arctic Ocean, such that the transport across the GSR remains stable or strengthens. This process seems already to have been initiated (Årthun et al., 2025) and is consistent with the updated time-series.

According to Table 1, the temperature of the Atlantic water is reduced from 8.40 °C to 7.37 °C and we have concluded that most of this is due to mixing with Arctic water over the IFR. It would be tempting to conclude that the heat transport relative

https://doi.org/10.5194/egusphere-2026-359
Preprint. Discussion started: 29 January 2026

to 0 °C has been similarly reduced by this mixing process, which would mean a reduction of around 10 %. That would, however, require that the volume transport is not affected in a compensatory manner. The amount of cooling is likely linked to the amount of Arctic water over the ridge and to the overflow across the ridge, but according to Hansen et al. (2010) and Olsen et al. (2016), the volume transport of the IF-inflow is also linked to the overflow. Conclusions as to the effect of mixing with colder Arctic waters on the heat transport would therefore be premature at this stage.

7. Summary and implications

The main aim of this study was to explain the temperature and salinity of the IF-inflow as it passes through the monitoring N-section and continues further into the Arctic Mediterranean. Our results indicate three main controlling processes: i) variations of the Subpolar Gyre (SPG) intrusion into the Iceland Basin, ii) global warming, iii) water mass modification during the crossing of the Iceland-Faroe Ridge (IFR). Air-Sea interaction over the IFR only has a small effect on the water mass modifications.

We find, that the salinity of the water approaching the IFR is mainly determined by the variable intrusion of the SPG into the Iceland Basin. An index quantifying this intrusion explains 69 % of the variance of the salinity with a lag of 3 years. SPG-intrusion also affects the temperature of the water approaching the IFR, but the explanatory power increases substantially when accounting for global warming.

SPG-intrusion and global warming, thus, control the temporal variations of the properties of the water approaching the IFR and these variations are to a large extent propagated across the IFR so that they also control the temporal variations of transport-weighted temperature and salinity through the N-section on decadal time scales. The average values for temperature and salinity are, however, strongly modified as the water crosses the ridge with a cooling of at least 1 °C and a freshening of more than 0.1 g kg^{-1}. These modifications are primarily caused by admixture of cold low-salinity water of Arctic origin into the Atlantic water mass. Without any detailed analysis of source waters and processes, we find the resulting water mass passing through the N-section may be seen as a mixture of original Atlantic water from west of the ridge and water from the upper 100 m east of Iceland in a 3 to 1 ratio.

Our results have some important implications. They show that this branch of the AMOC has actually strengthened slightly over the observational period and there are – in contrast to projected AMOC decline – no signs of a weakening.

The freshening of the IF-inflow implies a reduced potential for dense-water formation. The deep waters of the Arctic Mediterranean have salinities around 35.05 g kg^{-1}. Before crossing the IFR, the Atlantic water has salinities that are 0.35–0.45 g kg^{-1} above this. After crossing, this difference has been reduced by 0.1 g kg^{-1}. Since the density at low temperature is strongly dependent on salinity, this reduction severely impacts the potential for increasing the density of the IF-inflow waters to levels approaching the deep water density. This also affects the relative importance of the two main inflow branches as regards dense-water formation. Already before crossing the IFR, the IF-inflow has lower average salinities than the inflow through the Faroe-

https://doi.org/10.5194/egusphere-2026-359
Preprint. Discussion started: 29 January 2026

Shetland Channel and therefore lower potential for dense-water formation. After crossing, the salinity difference between the two inflow branches has increased.

Understanding the processes controlling the properties of Atlantic water that enters the Nordic Seas is important for validating and improving ocean and climate models as a whole. As such, our study indirectly strengthens the ability to produce more realistic forecasts of AMOC related changes in a warming climate.

https://doi.org/10.5194/egusphere-2026-359
Preprint. Discussion started: 29 January 2026

Author contributions

GE coordinated and performed most of the analysis and manuscript writing. BH assisted with analysis and writing. KMHL and SRÓ provided data and assisted with writing. SMO and AMUG assisted with writing.

Competing interests

The authors have no competing interests.

Acknowledgements

We thank all scientific and technical staff as well as captain and crew on all research vessels who performed the hydrographic observations and deployed the drifters. Likewise, we thank colleagues at FAMRI for all kind of support while performing this research and writing the paper. Thanks to Ilana Schiller-Weiss for comments on the draft manuscript. Sólvá K. Eliasen kindly provided the SST map in Figure 1. The observations at the N-section have been supported by the Danish Ministry of Climate, Energy and Utilities through its climate support program to the Arctic.

Financial support

KMHL and SMO are supported by Ocean observations and indicators for climate and assessments, ObsSea4Clim, Grant agreement ID: 101136548 (https://doi.org/10.3030/101136548), internal contribution Nr. 42

This research is part of the Faroe-AMOC project (https://www.pure.fo/en/projects/the-atlantic-meridional-overturning-circulation-in-the-waters-sur/), which received funding from the National Centre for Climate Research (NCKF – hosted at the Danish Meteorological Institute) and the Research Council Faroe Islands.

References

Arias, P. A., Bellouin, N., Coppola, E., Jones, R. G., Krinner, G., Marotzke, J., Naik, V., Palmer, M. D., Plattner, G.-K., Rogelj, J., Rojas, M., Sillmann, J., Storelvmo, T., Thorne, P. W., Trewin, B., Achuta Rao, K., Adhikary, B., Allan, R. P., Armour, K., Bala, G., Barimalala, R., Berger, S., Canadell, J. G., Cassou, C., Cherchi, A., Collins, W., Collins, W. D., Connors, S. L., Corti, S., Cruz, F., Dentener, F. J., Dereczynski, C., Di Luca, A., Diongue Niang, A., Doblas-Reyes, F. J., Dosio, A., Douville, H., Engelbrecht, F., Eyring, V., Fischer, E., Forster, P., Fox-Kemper, B., Fuglestvedt, J. S., Fyfe, J. C., Gillett, N. P., Goldfarb, L., Gorodetskaya, I., Gutierrez, J. M., Hamdi, R., Hawkins, E., Hewitt, H. T., Hope, P., Islam, A. S., Jones, C., Kaufman, D. S., Kopp, R. E., Kosaka, Y., Kossin, J., Krakovska, S., Lee, J.-Y., Li, J., Mauritsen, T., Maycock, T. K., Meinshausen, M., Min,

https://doi.org/10.5194/egusphere-2026-359
Preprint. Discussion started: 29 January 2026

S.-K., Monteiro, P. M. S., Ngo-Duc, T., Otto, F., Pinto, I., Pirani, A., Raghavan, K., Ranasinghe, R., Ruane, A. C., Ruiz, L., Sallée, J.-B., Samset, B. H., Sathyendranath, S., Seneviratne, S. I., Sörensson, A. A., Szopa, S., Takayabu, I., Tréguier, A.-M., van den Hurk, B., Vautard, R., von Schuckmann, K., Zaehle, S., Zhang, X., and Zickfeld, K.: Technical Summary, in: Climate Change 2021: The Physical Science Basis. Contribution of Working Group I to the Sixth Assessment Report of the Intergovernmental Panel on Climate Change, edited by: Masson-Delmotte, V., Zhai, P., Pirani, A., Connors, S. L., Péan, C., Berger, S., Caud, N., Chen, Y., Goldfarb, Z., Gomis, M. I., Huang, M., Leitzell, K., Lonnoy, E., Matthews, J. B. R., Maycock, T. K., Waterfield, T., Yelekçi, O., Yu, R., and Zhou, B., Cambridge University Press, Cambridge, United Kingdom and New York, NY, USA, 33–144, https://doi.org/10.1017/9781009157896.002, 2021.

Årthun, M., Eldevik, T., Viste, E., Drange, H., Furevik, T., Johnson, H. L., and Keenlyside, N. S.: Skillful prediction of northern climate provided by the ocean, Nat. Commun., 8, https://doi.org/10.1038/NCOMMS15875, 2017.

Årthun, M., Brakstad, A., Dörr, J., Johnson, H. L., Mans, C., Semper, S., and Våge, K.: Atlantification drives recent strengthening of the Arctic overturning circulation, Sci. Adv., 11, eadu1794, https://doi.org/10.1126/SCIADV.ADU1794, 2025.

Beaird, N. L., Rhines, P. B., and Eriksen, C. C.: Overflow waters at the Iceland-Faroe Ridge observed in multiyear seaglider surveys, J. Phys. Oceanogr., 43, 2334–2351, https://doi.org/10.1175/JPO-D-13-029.1, 2013.

Beaird, N. L., Rhines, P. B., and Eriksen, C. C.: Observations of seasonal subduction at the Iceland-Faroe Front, J. Geophys. Res.-Oceans, 121, 4026–4040, https://doi.org/10.1002/2015JC011501, 2016.

Biri, S. and Klein, B.: North Atlantic Sub-Polar Gyre Climate Index: A New Approach, J. Geophys. Res.-Oceans, 124, 4222–4237, https://doi.org/10.1029/2018JC014822, 2019.

Brambilla, E. and Talley, L. D.: Surface drifter exchange between the North Atlantic subtropical and subpolar gyres, J. Geophys. Res.-Oceans, 111, https://doi.org/10.1029/2005JC003146, 2006.

Bretones, A., Nisancioglu, K. H., Jensen, M. F., Brakstad, A., and Yang, S.: Transient Increase in Arctic Deep-Water Formation and Ocean Circulation under Sea Ice Retreat, J. Climate, 35, 109–124, https://doi.org/10.1175/JCLI-D-21-0152.1, 2022.

Buckley, M. W. and Marshall, J.: Observations, inferences, and mechanisms of the Atlantic Meridional Overturning Circulation: A review, Reviews of Geophysics, 54, 5–63, https://doi.org/10.1002/2015RG000493, 2016.

Childers, K. H., Flagg, C. N., and Rossby, T.: Direct velocity observations of volume flux between Iceland and the Shetland Islands, J. Geophys. Res.-Oceans, 119, 5934–5944, https://doi.org/10.1002/2014JC009946, 2014.

Childers, K. H., Flagg, C. N., Rossby, T., and Schrum, C.: Directly measured currents and estimated transport pathways of Atlantic Water between 59.58N and the Iceland-Faroes-Scotland Ridge, Tellus A: Dynamic Meteorology and Oceanography, 67, 28067, https://doi.org/10.3402/tellusa.v67.28067, 2015.

Fogelqvist, E., Blindheim, J., Tanhua, T., Østerhus, S., Buch, E., and Rey, F.: Greenland–Scotland overflow studied by hydro-chemical multivariate analysis, Deep-Sea Res. Pt. I, 50, 73–102, https://doi.org/10.1016/S0967-0637(02)00131-0, 2003.

https://doi.org/10.5194/egusphere-2026-359
Preprint. Discussion started: 29 January 2026

Foukal, N. P. and Lozier, M. S.: Assessing variability in the size and strength of the North Atlantic subpolar gyre, J. Geophys. Res.-Oceans, 122, 6295–6308, https://doi.org/10.1002/2017JC012798, 2017.

Fratantoni, D. M.: North Atlantic surface circulation during the 1990's observed with satellite-tracked drifters, J. Geophys. Res.-Oceans, 106, 22067–22093, https://doi.org/10.1029/2000JC000730, 2001.

Häkkinen, S. and Rhines, P. B.: Decline of Subpolar North Atlantic Circulation during the 1990s, Science, 304, 555–559, https://doi.org/10.1126/SCIENCE.1094917, 2004.

Hansen, B. and Meincke, J.: Eddies and meanders in the Iceland-Faroe Ridge area, Deep-Sea Res. Pt. A., 26, 1067–1082, https://doi.org/10.1016/0198-0149(79)90048-7, 1979.

Hansen, B. and Østerhus, S.: North Atlantic-Nordic Seas exchanges, Prog. Oceanogr., 45, 109–208, https://doi.org/10.1016/S0079-6611(99)00052-X, 2000.

Hansen, B., Hátún, H., Kristiansen, R., Olsen, S. M., and Østerhus, S.: Stability and forcing of the Iceland-Faroe inflow of water, heat, and salt to the Arctic, Ocean Sci., 6, 1013–1026, https://doi.org/10.5194/OS-6-1013-2010, 2010.

Hansen, B., Larsen, K. M. H., Hátún, H., Kristiansen, R., Mortensen, E., and Østerhus, S.: Transport of volume, heat, and salt towards the Arctic in the Faroe Current 1993-2013, Ocean Sci., 11, 743–757, https://doi.org/10.5194/os-11-743-2015, 2015.

Hansen, B., Larsen, K. M. H., Hátún, H., Olsen, S. M., Gierisch, A. M. U., Østerhus, S., and Ólafsdóttir, S. R.: The Iceland-Faroe warm-water flow towards the Arctic estimated from satellite altimetry and in situ observations, Ocean Sci., 19, 1225–1252, https://doi.org/10.5194/os-19-1225-2023, 2023.

Hátún, H. and Chafik, L.: On the Recent Ambiguity of the North Atlantic Subpolar Gyre Index, J. Geophys. Res.-Oceans, 123, 5072–5076, https://doi.org/10.1029/2018JC014101, 2018.

Hátún, H., Sande, A. B., Drange, H., Hansen, B., and Valdimarsson, H.: Influence of the Atlantic Subpolar Gyre on the Thermohaline Circulation, Science, 309, 1841–1844, https://doi.org/10.1126/SCIENCE.1114777, 2005.

Helland-Hansen, B. and Nansen, F.: The Norwegian Sea, its physical oceanography. Based on the Norwegian researches 1900–1904, Report on Norwegian fishery and marine-investigations, 2, 390 pp+25 plates. 1909.

Holliday, N. P., Bersch, M., Berx, B., Chafik, L., Cunningham, S., Florindo-López, C., Hátún, H., Johns, W., Josey, S. A., Larsen, K. M. H., Mulet, S., Oltmanns, M., Reverdin, G., Rossby, T., Thierry, V., Valdimarsson, H., and Yashayaev, I.: Ocean circulation causes the largest freshening event for 120 years in eastern subpolar North Atlantic, Nat. Commun., 11, 585, https://doi.org/10.1038/s41467-020-14474-y, 2020.

Jakobsen, P. K., Ribergaard, M. H., Quadfasel, D., Schmith, T., and Hughes, C. W.: Near-surface circulation in the northern North Atlantic as inferred from Lagrangian drifters: Variability from the mesoscale to interannual, J. Geophys. Res, 108, 3251, https://doi.org/10.1029/2002JC001554, 2003.

Jochumsen, K., Schnurr, S. M., and Quadfasel, D.: Bottom temperature and salinity distribution and its variability around Iceland, Deep-Sea Res. Pt. I, 111, 79–90, https://doi.org/10.1016/J.DSR.2016.02.009, 2016.

Knudsen, M.: Den Danske Ingolf-expedition., Bianco Lunos Kgl Hof-Bogtrykkeri (F. Dreyer), København, 1, 21–154, 1898.

https://doi.org/10.5194/egusphere-2026-359
Preprint. Discussion started: 29 January 2026

Koman, G., Johns, W. E., Houk, A., Houpert, L., and Li, F.: Circulation and overturning in the eastern North Atlantic subpolar gyre, Prog. Oceanogr., 208, 102884, https://doi.org/10.1016/j.pocean.2022.102884, 2022.

Larsen, K. M. H., Hátún, H., Hansen, B., and Kristiansen, R.: Atlantic water in the Faroe area: sources and variability, ICES J. Mar. Sci., 69, 802–808, https://doi.org/10.1093/icesjms/fss028, 2012.

Logemann, K., Ólafsson, J., Snorrason, Á., Valdimarsson, H., and Marteinsdóttir, G.: The circulation of Icelandic waters-a modelling study, Ocean Sci., 9, 931–955, https://doi.org/10.5194/os-9-931-2013, 2013.

de Marez, C., Ruiz-Angulo, A., and Gula, J.: Mesoscale Induced Vertical Fluxes Over the Iceland-Faroe Ridge, Geophys. Res. Lett., 52, https://doi.org/10.1029/2025GL115520, 2025.

Meincke, J.: The hydrographic section along the Iceland–Faroe Ridge carried out by R.V. "Anton Dohrn" in 1959–1971, Berichte der Deutschen Wissenschaftlichen Kommission für Meeresforschung, 22, 372–384, 1972.

Meincke, J.: On the distribution of low salinity intermediate waters around the Faroes, Deutsche Hydrographische Zeitschrift, 31, 50–64, https://doi.org/10.1007/BF02226000, 1978.

Mulet, S., Rio, M. H., Etienne, H., Artana, C., Cancet, M., Dibarboure, G., Feng, H., Husson, R., Picot, N., Provost, C., and Strub, P. T.: The new CNES-CLS18 global mean dynamic topography, Ocean Sci., 17, 789–808, https://doi.org/10.5194/OS-17-789-2021, 2021.

Olsen, S. M., Hansen, B., Østerhus, S., Quadfasel, D., and Valdimarsson, H.: Biased thermohaline exchanges with the Arctic across the Iceland–Faroe Ridge in ocean climate models, Ocean Sci., 12, 545–560, https://doi.org/10.5194/os-12-545-2016, 2016.

Orvik, K. A. and Niiler, P.: Major pathways of Atlantic water in the northern North Atlantic and Nordic Seas toward Arctic, Geophys. Res. Lett., 29, https://doi.org/10.1029/2002GL015002, 2002.

Østerhus, S., Woodgate, R., Valdimarsson, H., Turrell, B., De Steur, L., Quadfasel, D., Olsen, S. M., Moritz, M., Lee, C. M., Larsen, K. M. H., Jónsson, S., Johnson, C., Jochumsen, K., Hansen, B., Curry, B., Cunningham, S., and Berx, B.: Arctic Mediterranean exchanges: A consistent volume budget and trends in transports from two decades of observations, Ocean Sci., 15, 379–399, https://doi.org/10.5194/OS-15-379-2019, 2019.

Perkins, H., Hopkins, T. S., Malmberg, S.-A., Poulain, P.-M., and Warn-Varnas, A.: Oceanographic conditions east of Iceland, J. Geophys. Res., 103, 531–552, https://doi.org/10.1029/98JC00890, 1998.

Poulain, P. M., Gerin, R., Mauri, E., and Pennel, R.: Wind Effects on Drogued and Undrogued Drifters in the Eastern Mediterranean, J. Atmos. Ocean. Tech., 26, 1144–1156, https://doi.org/10.1175/2008JTECHO618.1, 2009.

Read, J. F. and Pollard, R. T.: Water Masses in the Region of the Iceland-Færoes Front, J. Phys. Oceanogr., 22, https://doi.org/10.1175/1520-0485(1992)022<1365:WMITRO>2.0.CO;2, 1992.

Rossby, T., Prater, M. D., and Søiland, H.: Pathways of inflow and dispersion of warm waters in the Nordic seas, J. Geophys. Res-Oceans., 114, C04011, https://doi.org/10.1029/2008JC005073, 2009.

Sutton, R. T. and Allen, M. R.: Decadal predictability of North Atlantic sea surface temperature and climate, Nature, 388, 563–567, https://doi.org/10.1038/41523, 1997.

https://doi.org/10.5194/egusphere-2026-359
Preprint. Discussion started: 29 January 2026

Tait, J. B.: The Iceland-Faroe Ridge International (ICES) “Overflow” Expedition, May-June 1960, Rapports et Procès-Verbaux des Rèunions du Conseil International pour l’Exploration de la Mer, 157, 71, 1967.